



Design, synthesis, and evaluation of imidazo[4,5-c]pyridin-4-one derivatives with dual activity at angiotensin II type 1 receptor and peroxisome proliferator-activated receptor- γ

Agustin Casimiro-Garcia^{a,*}, Ronald J. Heemstra^b, Christopher F. Bigge^b, Jing Chen^b, Fred A. Ciske^b, Jo Ann Davis^c, Teresa Ellis^b, Nadia Esmaeil^b, Declan Flynn^b, Seungil Han^b, Mehran Jalaie^c, Jeffrey F. Ohren^b, Noel A. Powell^b

^a Worldwide Medicinal Chemistry, Pfizer Worldwide Research and Development, 200 Cambridgepark Drive, Cambridge, MA 02140, USA

^b Pfizer Worldwide Research and Development, Eastern Point Rd, Groton, CT 06340, USA

^c Pfizer Worldwide Research and Development, 10770 Science Center Drive, San Diego, CA 92121, USA

ARTICLE INFO

Article history:

Received 9 October 2012

Revised 15 November 2012

Accepted 20 November 2012

Available online 1 December 2012

Keywords:

Angiotensin

Peroxisome proliferator-activated receptor

PPAR γ

Hypertension

Metabolic syndrome

ABSTRACT

Identification of a series of imidazo[4,5-c]pyridin-4-one derivatives that act as dual angiotensin II type 1 (AT1) receptor antagonists and peroxisome proliferator-activated receptor- γ (PPAR γ) partial agonists is described. Starting from a known AT1 antagonist template, conformational restriction was introduced by incorporation of an indane ring that when combined with appropriate substitution at the imidazo[4,5-c]pyridin-4-one provided novel series **5** possessing the desired dual activity. The mode of interaction of this series with PPAR γ was corroborated through the X-ray crystal structure of **12b** bound to the human PPAR γ ligand binding domain. Modulation of activity at both receptors through substitution at the pyridone nitrogen led to the identification of potent dual AT1 antagonists/PPAR γ partial agonists. Among them, **21b** was identified possessing potent dual pharmacology (AT1 IC₅₀ = 7 nM; PPAR γ EC₅₀ = 295 nM, 27% max) and good ADME properties.

© 2012 Elsevier Ltd. All rights reserved.

Hypertension is commonly associated with an array of other factors including abdominal obesity, insulin resistance, elevated plasma glucose, and dyslipidemia that collectively are often referred to as the metabolic syndrome.^{1,2} Currently, there are no approved drugs that can reduce all of the risk factors associated with the metabolic syndrome. Therefore, there is a growing interest in therapeutic approaches that simultaneously target multiple factors with a single therapy. Angiotensin II type 1 (AT1)[†] receptor blockers (ARBs) are clinically effective, well tolerated agents for the treatment of hypertension. Among them, telmisartan (**1**, Fig. 1), is not only a potent and selective AT1 receptor antagonist, but also, it was reported with partial activity at the nuclear hormone receptor peroxisome proliferator-activated receptor- γ (PPAR γ).^{3,4} Telmisartan has a well documented efficacy in blood pressure (BP) reduction,⁵ and has also demonstrated improvements in glucose and lipid metabolism in small clinical trials.^{6,7} The improvements observed in patients taking telmisartan could be reasonably attributed to its partial activity at

PPAR γ . More recently, telmisartan was shown to be more effective than valsartan, an ARB without PPAR γ activity, in reducing body weight and providing better renal protection in a rodent model of the metabolic syndrome.⁸ These effects of telmisartan have also been attributed to its partial PPAR γ activity.^{8,9} A pharmaceutical agent possessing the dual pharmacology of AT1 receptor antagonism and partial PPAR γ agonism could potentially treat several recognized cardiovascular risk factors including hypertension, insulin resistance and hypertriglyceridemia in patients with metabolic syndrome. Our group recently reported a series of imidazo[4,5-b]pyridines **2** possessing this dual pharmacology.^{10–12} This series is exemplified with **3** that was identified as a potent angiotensin II type I receptor blocker (IC₅₀ = 1.6 nM) with partial PPAR γ agonism (EC₅₀ = 212 nM, 31% max) and oral bioavailability in rat.¹¹ The dual pharmacology of **3** was demonstrated in animal models of hypertension (spontaneously hypertensive rat - SHR) and insulin resistance (Zucker diabetic fatty rat - ZDF). The potent selective antagonism of the AT1 receptor translated into highly effective BP lowering in the SHR. A single dose of 10 mg/kg produced BP lowering for a full 24 h equivalent to the effect observed with telmisartan. The potent, partial activation of the PPAR γ receptor translated into dose dependent efficacy in the male ZDF rat with glycemic improvements equivalent to that of pioglitazone with a significantly reduced incidence of weight gain.

* Corresponding author.

E-mail address: agustin.casimiro-garcia@pfizer.com (A. Casimiro-Garcia).

[†] Abbreviations: ARB, angiotensin receptor blocker; AT1, angiotensin II type 1 receptor; BP, blood pressure; BW, body weight; CV, cardiovascular; LBD, ligand binding domain; PPAR γ , peroxisome proliferator-activated receptor- γ ; SHR, spontaneously hypertensive rat; ZDF, Zucker diabetic fatty rat.

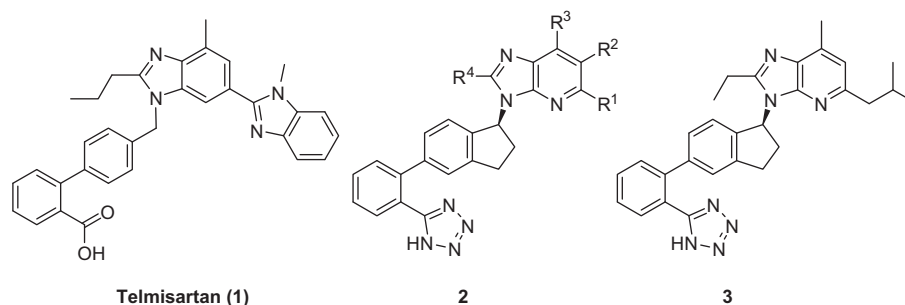


Figure 1. Chemical structures of telmisartan (**1**), imidazo[4,5-*b*]pyridines series **2**, and **3**.

More interestingly, plasma concentrations achieving significant efficacy were within three-fold in the SHR and ZDF models for **3** demonstrating the potential utility of this compound in treating multiple risk factors at a single dose level.

A complementary series possessing the desired dual pharmacology of AT1 antagonism and partial PPAR γ agonism was desired. From a strategic point of view, we were interested in the identification of a second series possessing a relatively similar dual activity profile to that obtained with **3**. This profile was already shown to provide significant efficacy in animal models of both hypertension and insulin resistance at a single dose level. During the course of our research with the imidazo[4,5-*b*]pyridines series **2**, it was demonstrated that conformational restriction derived from the indane ring is required for PPAR γ activity. In addition, substitution at R¹ in scaffold **2** (Fig. 1) was identified as an optimal position to modulate activity at both AT1 and PPAR γ receptors. Examination of known ARBs revealed a number of scaffolds that might be used to build the dual activity.¹³ Among them, a series of imidazo[4,5-*c*]pyridin-4-one derivatives **4** (Fig. 2) reported as potent AT1 receptor antagonists appeared as potential starting points.¹⁴ It was envisioned that conformational restriction obtained by introduction of an indane ring, and appropriate substitution at the imidazopyridone ring could provide novel series **5** possessing the desired dual activity of AT1 antagonism and partial PPAR γ agonism. Based on our previous work with series **2**,¹¹ only compounds with the *S* configuration at the indane asymmetric center were planned in the new series **5**. In this Letter, the design, synthesis, and in vitro biological evaluation of this novel series of imidazo[4,5-*c*]pyridin-4-ones **5** are described.¹⁵

The synthesis of imidazo[4,5-*c*]pyridin-4-one analogs incorporating an indane ring is depicted in Scheme 1. The heterocyclic head group **6** was prepared as previously described,¹⁴ while (*R*)-5-bromo-1-indanol (**7**) was obtained via catalytic enantioselective reduction of 5-bromo-1-indanone using conditions previously reported by our group.¹¹ Mitsunobu reaction of indanol **7** with imidazopyridone **6** utilizing the conditions of diethyl azodicarboxylate

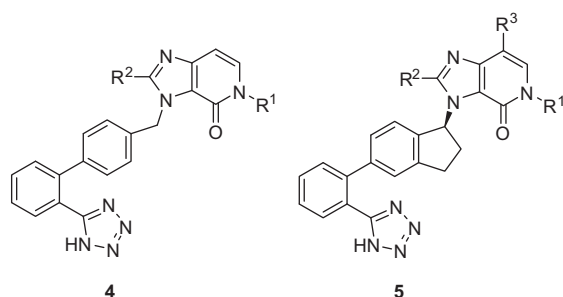
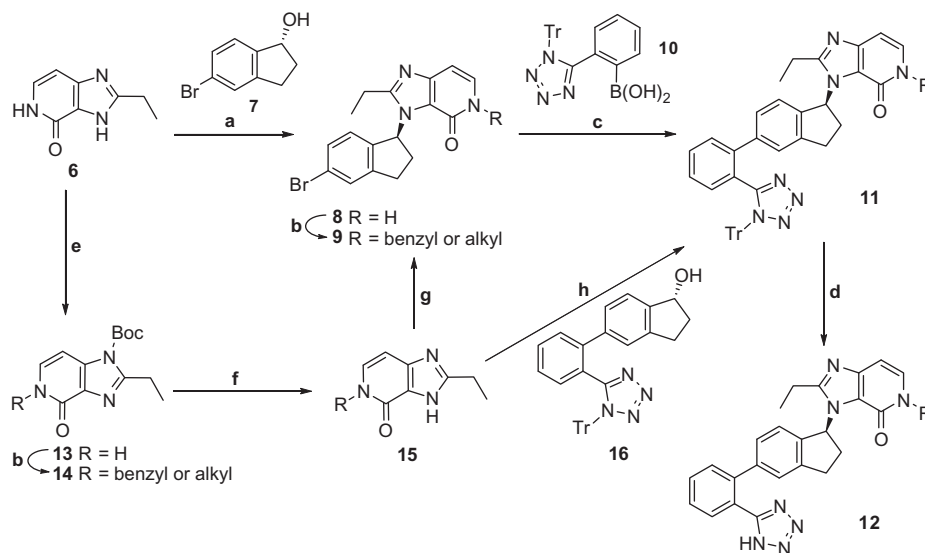


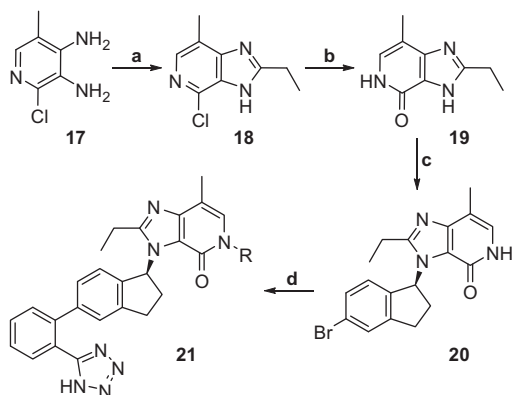
Figure 2. Chemical structure of known series of imidazo[4,5-*c*]pyridin-4-one AT1 antagonists **4** and new series **5**.

and triphenylphosphine in THF provided the desired *N*-indanylimidazopyridone **8**, albeit in low and irreproducible yields. The problem with this transformation was likely derived from the low solubility of the imidazopyridone **6** in the reaction mixture. Efforts to improve the yield of this step were unsuccessful. The regiochemistry of substitution in **8** was established through 2-D NMR studies. X-ray crystallography studies described later in this report further supported the structural assignment. Suzuki cross-coupling of bromide **8** with boronic acid **10**¹⁶ in the presence of catalytic palladium acetate, triphenylphosphine, and potassium carbonate in DME-water gave **11a** (*R* = *H*). Removal of the trityl group under the conditions of 3 M HCl in acetone afforded tetrazole **12a** (*R* = *H*). Benzoylation of **8** to provide bromide **9b** (*R* = benzyl), followed by Suzuki cross-coupling of this bromide with boronic acid **10**, and removal of the trityl protecting group provided **12b** (*R* = benzyl). The synthetic route utilized for the preparation of **12a** and **12b** was not adequate to support efforts to further explore modifications in this series and led us to investigate an alternative route. Selective protection of the imidazole NH group in **6** using Boc anhydride and catalytic DMAP gave **13**. The position of the Boc group in **13** was confirmed through 2-D NMR studies. Alkylation of **13** with appropriate alkyl-, or benzyl halides utilizing potassium *tert*-butoxide in dry THF provided **14**. Boc group removal under the conditions of TFA in DCM gave **15**. The Mitsunobu reaction of **15** with (*R*)-5-bromo-1-indanol (**7**) was then investigated. Optimal conditions consisted in performing this reaction in the presence of di-*tert*-butyl azodicarboxylate and trimethylphosphine in THF to give the desired *N*-indanylimidazopyridones **9** (*R* = substituted benzyl or alkyl) in satisfactory and reproducible yields. Interestingly, the solubility of the *N*-substituted imidazopyridones **15** was noticeably better than for the unsubstituted **6** under these conditions. The remaining of the synthesis followed the same steps as previously described for bromide **9b**. In this manner, additional tetrazoles **12** incorporating substituted benzyl or alkyl groups at the pyridone nitrogen were obtained. The modified conditions were also applied for the Mitsunobu reaction between **15** and the more elaborated and previously reported indanol **16**¹¹ to provide in a single step trityl-protected tetrazoles **11** in acceptable yields that could be converted into the desired tetrazoles **12** (*R* = substituted benzyl or alkyl) after trityl group removal.

Selected analogs with a methyl group at the C-7 position of the imidazo[4,5-*c*]pyridin-4-one were prepared according to Scheme 2. Heating a mixture of diaminopyridine **17**¹⁷ with propionic acid in the presence of polyphosphoric acid provided imidazopyridine **18**. After purification, **18** was treated with 96% formic acid and the mixture heated under reflux to provide imidazopyridone **19**. Mitsunobu reaction of **19** with indanol **7** was accomplished by running this reaction in the presence of di-*tert*-butyl azodicarboxylate and trimethylphosphine in THF to give **20** in satisfactory yields. To complete the synthesis, *N*-benzylation, followed by Suzuki cross-coupling and removal of the trityl group as described above provided tetrazoles **21**.



Scheme 1. Synthesis of imidazo[4,5-c]pyridin-4-one analogs. Reagents and conditions: (a) **7**, DEAD, Ph₃P, THF, 0–25 °C, 6–10%; (b) RBr, KOtBu, THF, 40–50%; (c) **10**, Pd(OAc)₂, PPh₃, K₂CO₃, DME–H₂O, 80 °C, 75–85%; (d) 3 M HCl, acetone, 75–95%; (e) Boc₂O, DMAP, Et₃N, THF, 49%; (f) TFA, DCM; (g) **7**, D_tBAD, Me₃P, THF, –78 to 25 °C, 70–80%, 2 steps; (h) **16**, D_tBAD, Me₃P, THF, –78 to 25 °C, 40–50%.



Scheme 2. Synthesis of C-7 methyl imidazo[4,5-c]pyridin-4-one analogs. Reagents and conditions: (a) propionic acid, PPA, 80 °C, 76%; (b) 96% formic acid, reflux, 92%; (c) **7**, D_tBAD, Me₃P, THF, –78 to 25 °C, 29%; (d) (i): RBr, KOtBu, THF, rt; (ii): **10**, Pd(OAc)₂, PPh₃, K₂CO₃, DME–H₂O, 80 °C; iii: 3 M HCl, acetone, 66%, 3 steps.

The new compounds were evaluated for affinity for the AT1 receptor utilizing human recombinant AT1 receptors in a competition radioligand binding assay with [¹²⁵I]Tyr⁴-Sar¹,Ile⁸-Angiotensin II. The IC₅₀ values of the imidazo[4,5-c]pyridin-4-one analogs are displayed in Tables 1 and 2. Activation of human PPAR γ was determined using a chimeric receptor (PPAR γ Ligand Binding Domain (LBD)/ Gal4 DNA Binding Domain) transactivation assay. The EC₅₀ values and the percent of maximal activation with darglitazone¹⁸ as a reference full agonist (defined as 100% effect) are also presented in Tables 1 and 2. Telmisartan, pioglitazone, and **3** are included as reference compounds.

Our initial efforts were directed at determining the impact of the indane ring on the AT1 activity of the new scaffold, and to investigate if PPAR γ activity could be obtained. Imidazopyridones **12a** and **12c** were synthesized early and compared with previously reported AT1 receptor antagonists.¹⁴ While results obtained with **12a** suggested loss of AT1 activity with introduction of the indane ring, substitution on the pyridone nitrogen in **12c** demonstrated that this activity could be recovered with appropriate substitution (Table 1). However, no PPAR γ activity was observed with these two

Table 1
AT1 and PPAR γ transactivation activity of imidazo[4,5-c]pyridin-4-one derivatives **12a–g** and reference compounds

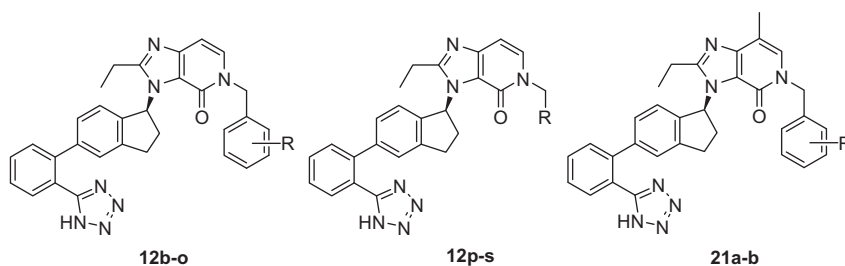
Compound	R	AT1 IC ₅₀ (nM)	h-PPAR γ EC ₅₀ (nM) ^a (% max) ^b
Telmisartan		0.49	1520 (33)
Pioglitazone		–	1280 (80)
3		1.6	212 (31)
12a	H	593	>100,000
12b	CH ₂ Ph	12.7	292 (25)
12c	CH ₂ CON(CH ₃) ₂	24.4	>100,000
12d	CH ₂ COOCH ₂ Ph	19.8	1250 (27)
12e	CH ₂ COOH	348	>100,000
12f	CH ₂ CH(CH ₃) ₂	19.4	1710 (23)
12g	CH ₂ c-hexyl	41	942 (26)

^a TA (transactivation assay). Mean value of at least two determinations.

^b The maximal efficacy of darglitazone in the PPAR γ activation assay was defined as 100%. All compounds were prepared as the (S)-enantiomer.

compounds. Efforts were focused to investigate additional substituents at the pyridone nitrogen, including both lipophilic and polar groups. These modifications led not only to improve AT1 activity, but also to achieve the desired dual activity as several of the new derivatives demonstrated PPAR γ activity. Among this set of compounds, benzyl analog **12b** represented the most potent analog (AT1 IC₅₀ = 12.7 nM, PPAR γ EC₅₀ = 292 nM, 25% max) and provided an interesting lead for further investigation. Benzyl analog **12b** was tested in PPAR α and PPAR β screens and showed no activity for these receptors (EC₅₀ >50,000 nM) thus confirming the selectivity of this scaffold for PPAR γ . We have observed similar selectivity results with our previously reported **3**.¹¹ The difference in AT1 and

Table 2
AT1 and PPAR γ transactivation activity of imidazo[4,5-c]pyridin-4-one derivatives **12b–s** and **21a–b**



Compound	R	AT1 IC ₅₀ (nM)	h-PPAR γ ^a EC ₅₀ (nM) (% max) ^b
12b	H	12.7	292 (25)
12h	2-F	37.7	103 (22)
12i	2-CH ₃	5.1	97 (20)
12j	2-CN	13.5	685 (24)
12k	2-CF ₃	94.1	187 (25)
12l	2-OCF ₃	29.3	20 (30)
12m	3-F	67.4	159 (20)
12n	3-CH ₃	36.9	108 (21)
12o	3-CF ₃	81.6	449 (19)
12p	2-Pyridyl	63.8	3580 (15)
12q	3-Pyridyl	45.2	3640 (32)
12r	4-Pyridyl	250	>25,000
12s	3,5-Dimethyl-4-isoxazolyl	63.4	4470 (14)
21a	2-CH ₃	6.8	42 (32)
21b	2-CN	7	295 (27)

^a TA (transactivation assay). Mean value of at least two determinations.

^b The maximal efficacy of darglitazone in the PPAR γ activation assay was defined as 100%. All compounds were prepared as the (*S*)-enantiomer.

PPAR γ activity observed when comparing **12a** with **12b** is quite drastic. It was known from the previous work reported on this class of AT1 antagonists that a benzyl group at the pyridone nitrogen had comparable AT1 activity to that of an unsubstituted pyridone analog.¹⁴ Thus, it appears that a benzyl, or other lipophilic substituent is required in the indane-based scaffold to achieve better affinity for the AT1 receptor. Based on the assumption that the new imidazo[4,5-c]pyridin-4-one scaffold would bind to PPAR γ in a similar mode to that of our previously reported series **2**, incorporation of lipophilic groups on the pyridone nitrogen of **12a** was expected to provide an improvement on PPAR γ activity. In our previous work with series **2**, it was observed that larger and more lipophilic R¹ substituents in **2** (Fig. 1) generally led to more potent PPAR γ agonists. The improved PPAR γ activity was likely derived from additional interactions with hydrophobic residues that surround this region of the molecule. The results obtained with **12b**, **12d**, **12f**, and **12g** showed this approach works in this scaffold to improve PPAR γ activity, as this set of compounds exhibited PPAR γ activity in an acceptable potency range.

The benzyl analog **12b** was the most potent compound in the initial set and an interesting lead for further investigation. Our approach to take advantage of this interesting compound was twofold. First, taking advantage of our experience in X-ray crystallography of PPAR γ agonists,^{11,19,20} efforts were directed at getting a crystal structure of **12b** bound to the PPAR γ ligand binding domain (LBD) that could be used to guide design. Second, a number of analogs incorporating modifications on the benzyl ring, as well as replacements of the benzyl group with heteroaryl rings were planned to gain a better knowledge of structural requirements for both AT1 and PPAR γ activity. The structure of the complex of **12b** bound to the human PPAR γ LBD was determined by X-ray crystallography at 2.02 Å resolution and is displayed in Fig. 3 (see Supplementary data S-Table 1 for X-ray data collection and structure refinement statistics).²¹ The mode of binding of **12b** resembled the mode of binding observed with our previous series

2 and differed from that observed with full PPAR γ agonists.^{19,20} The lipophilic benzyl group is projected into the AF-2 domain pocket of the receptor and interacts with the charge clamp residues and other residues in this region through non-polar, van der Waals interactions. The crystal structure also revealed that the acidic tetrazole motif is buried into the hydrophobic anterior of the receptor and makes an H-bond interaction between the N-1 of the tetrazole ring and the backbone NH of Ser342 (2.9 Å distance). An H-bond between N-2 of the tetrazole ring and Arg288 was observed with series **2**. This H-bond is absent in the structure of the complex of **12b** as this residue appears to be flexible and is positioned away from the ligand.

The crystallography results obtained with **12b** provided guidance for the selection and position of substituents incorporated on the phenyl ring of the benzyl group to improve interaction with PPAR γ . The C-2 position on the phenyl ring appeared optimal as a pocket in the receptor was identified surrounding this region of the ligand. Analogs incorporating small groups like CH₃, F, and CN on the benzyl ring were expected to be well tolerated. Analogs with substitution at other positions, as well as compounds with heteroaryl groups replacing the benzyl moiety were also planned. The results obtained with **12h–12l** containing small C-2 substituents showed that indeed this position can provide enhancements in PPAR γ potency (Table 2). This set of compounds showed potent PPAR γ activity, with **12l** (R = 2-OCF₃; EC₅₀ = 20 nM, 30% max) as the most potent analog in this set that represents >14-fold increase in PPAR γ potency over **12b**. Although only a limited set of heteroaryl rings were explored, the results obtained with **12p–12s** (Table 2) suggested a limited opportunity to replace the benzyl moiety with an heteroaryl group, as these compounds exhibited >10-fold drop in PPAR γ potency when compared to **12b**. The apparently limited toleration for the more polar heteroaryl rings was not expected, as the region surrounding the benzyl group of **12b** is not entirely lined with hydrophobic residues. There are several polar residues in PPAR γ near the benzyl group of **12b** that

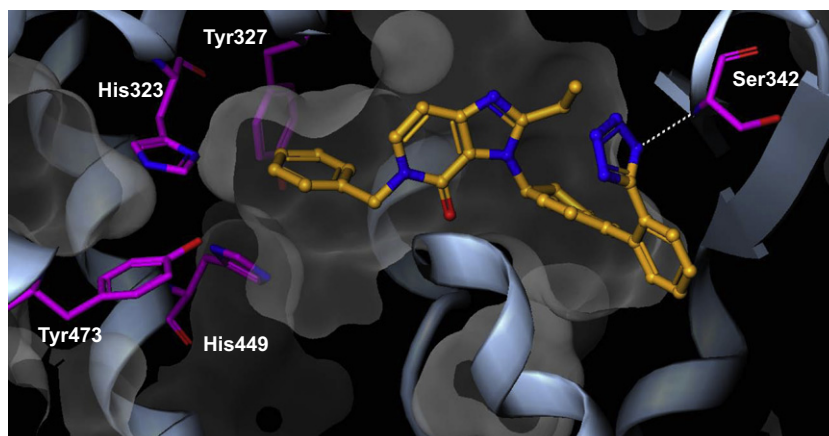


Figure 3. Three-dimensional representation of **12b** (gold) bound in the ligand binding pocket of human PPAR γ (blue ribbons and β -sheets with magenta residues). The compound wraps around helix 3 that lies in the middle. The benzyl group interacts through a number of hydrophobic interactions with the charge clamp residues and other residues in this region. Formation of an H-bond between N-1 of the tetrazole ring and the backbone NH of Ser342 (2.9 Å distance) was observed.

Table 3
In vitro ADME and physicochemical properties of selected analogs.

Compound	LogD ^a	HLM Cl _{int} (μL/min/mg)	PAMPA ^b (× 10 ⁻⁶ cm/sec)	Solubility ^c (μM)	DDI ^d (% inhibition)	
					3A4	2D6
12i	2.6	32.6	3.6	3.5	14	6
12j	1.7	14	10.7	11.7	31	11
21a	2.9	37.5	7.0	ND	3.5	4.5
21b	2.5 ^e	20.7	19	5.2	0	0

^a Experimental LogD.²²

^b Permeability determined using PAMPA.

^c Kinetic solubility.²³

^d Drug–drug interaction.²⁴

^e Calculated LogD value.

could accommodate heteroaryl groups. Other factors like higher desolvation penalty of the heteroaryl rings might explain the loss in PPAR γ potency observed with these compounds.

In contrast to the PPAR γ activity, improving AT1 activity was significantly more challenging. In general most of the substituents incorporated on the benzyl group, as well as the heteroaryl group replacements led to a drop in AT1 potency when compared to **12b** (Table 2). Two compounds were identified that provided moderate improvements over **12b**. **12i** (R = 2-CH₃) showed a modest improvement in potency at both receptors (AT1 IC₅₀ = 5.1 nM; EC₅₀ = 97 nM, 20% max). Another interesting analog was **12j** (R = 2-CN) that although it showed similar potency for AT1 and reduced potency for PPAR γ (AT1 IC₅₀ = 13.5 nM; EC₅₀ = 685 nM, 24% max) than **12b**, the presence of the more polar nitrile group at C-2 was interesting as it was predicted to provide advantages in terms of physicochemical and ADME properties. In an effort to further improve on these compounds, incorporation of a methyl group at C-7 of the imidazopyridone scaffold was pursued. This approach was based on results from our series **2** in which the methyl group at C-7 of the imidazopyridine ring was observed to enhance AT1 and PPAR γ potency. Both **21a** (AT1 IC₅₀ = 6.8 nM; EC₅₀ = 42 nM, 32% max) and **21b** (AT1 IC₅₀ = 7 nM; EC₅₀ = 295 nM, 27% max) were approximately equipotent to their corresponding analogs **12i** and **12j**. Although the number of compounds is limited, the results obtained with **21a** and **21b** suggested a limited opportunity to achieve a large improvement in potency with the methyl at C-7 position and demonstrated differences in SAR between the imidazopyridone scaffold and series **2**.

Selected physicochemical and in vitro ADME properties of analogs **12i**, **12j**, **21a** and **21b** are displayed in Table 3. The measured properties of **12j** and **21b** confirmed our expectations that the

polar nitrile group in these compounds would confer better properties. In particular, **21b** demonstrated moderate in vitro human liver microsomes intrinsic clearance, high permeability, moderate kinetic solubility, and low potential for drug–drug interactions for two major cytochrome P450 isoforms 3A4 and 2D6, while exhibiting potent activity at both receptors.

In summary, a new series of dual AT1 antagonists and partial PPAR γ agonists based on a imidazo[4,5-c]pyridin-4-one scaffold was discovered through modification of a known AT1 antagonist template. Our approach to build the desired dual activity consisted in utilizing conformational restriction derived from introduction of an indane ring and appropriate substitution at the imidazopyridone ring. This effort was further guided by the X-ray crystallography structure of **12b** bound to PPAR γ LBD that also served to confirm the mode of binding of this series with PPAR γ which differed from that observed with full PPAR γ agonists. It was interesting to observe that modulation of activity at both receptors could be accomplished through modification at a single position, the pyridone nitrogen. This work led to the identification of potent dual AT1 antagonists/PPAR γ partial agonists represented with **21b** that not only showed a potency profile at both receptors similar to some of the best compounds from our previously disclosed series **2**, but it also demonstrated good ADME and physicochemical properties.

Supplementary data

Supplementary data associated with this article can be found, in the online version, at <http://dx.doi.org/10.1016/j.bmcl.2012.11.088>.

References

1. Miranda, P. J.; DeFronzo, R. A.; Califf, R. M.; Guyton, J. R. *Am. Heart J.* **2005**, *149*, 33.
2. Grundy, S. M. *Nat. Rev. Drug Disc.* **2006**, *5*, 295.
3. Schupp, M.; Janke, J.; Clasen, R.; Unger, T.; Kintscher, U. *Circulation* **2004**, *109*, 2054.
4. Benson, S. C.; Pershadsingh, H. A.; Ho, C. I.; Chittiboyina, A.; Desai, P.; Pravenec, M.; Qi, N.; Wang, J.; Avery, M. A.; Kurtz, T. W. *Hypertension* **2004**, *43*, 993.
5. Goebel, M.; Clemenz, M.; Unger, T. *Expert Rev. Cardiovasc. Ther.* **2006**, *4*, 615.
6. Derosa, G.; Ragonesi, P. D.; Mugellini, A.; Ciccarelli, L.; Fogari, R. *Hypertens. Res.* **2004**, *27*, 457.
7. Vitale, C.; Mercurio, G.; Castiglioni, C.; Cornoldi, A.; Tulli, A.; Fini, M.; Volterrani, M.; Rosano, G. M. C. *Cardiovasc. Diabetol.* **2005**, *4*, 6.
8. Khan, M. A. H.; Imig, J. D. *Am. J. Hypertens.* **2011**, *24*, 816.
9. Sernia, C.; Brown, L. *Am. J. Hypertens.* **2011**, *24*, 739.
10. Casimiro-Garcia, A.; Bigge, C. F.; Chen, J.; Davis, J. A.; Dudley, D. A.; Edmunds, J. J.; Esmail, N.; Filzen, G.; Flynn, D.; Geyer, A.; Heemstra, R. J.; Jalaie, M.; Ohren, J. F.; Padalino, T.; Pulaski, J.; Schaum, R. P.; Stoner, C. L. In *Abstract of Papers, 239th American Chemical Society National Meeting, San Francisco, CA*, American Chemical Society, Washington, DC, 2010; MEDI-200.
11. Casimiro-Garcia, A.; Filzen, G. F.; Flynn, D.; Bigge, C. F.; Chen, J.; Davis, J. A.; Dudley, D. A.; Edmunds, J. J.; Esmail, N.; Geyer, A.; Heemstra, R. J.; Jalaie, M.; Ohren, J. F.; Ostroski, R.; Padalino, T.; Schaum, R. P.; Stoner, C. *J. Med. Chem.* **2011**, *54*, 4219.
12. Casimiro-Garcia, A.; Schaum, R. P.; Flynn, D.; Bigge, C. F.; Bolton, G.; Chen, J.; Cohen, L.; Davis, J. A.; Dudley, D. A.; Edmunds, J. J.; Ellis, T.; Erasga, N.; Esmail, N.; Heemstra, R. J.; Jalaie, M.; Lee, C.; Ohren, J. F.; Ostroski, R.; Risley, H. L.; Tugnait, M. Presented at the 244th American Society National Meeting, Philadelphia, PA, August 2012; MEDI-250.
13. Middlemiss, D.; Watson, S. P. *Tetrahedron* **1994**, *50*, 13049.
14. Mederski, W. W. K. R.; Dorsch, D.; Bokel, H.-H.; Beier, N.; Lues, I.; Schelling, P. *J. Med. Chem.* **1994**, *37*, 1632.
15. A preliminary report was presented recently: Casimiro-Garcia, A.; Bigge, C. F.; Chen, J.; Ciske, F. A.; Davis, J. A.; Edmunds, J. J.; Esmail, N.; Flynn, D.; Heemstra, R. J.; Jalaie, M.; Ohren, J. F.; Padalino, T.; Powell, N. A.; Pulaski, J. In *Abstract of Papers, 239th American Chemical Society National Meeting, San Francisco, CA*: American Chemical Society, Washington, DC, 2010; MEDI-505.
16. Lo, Y. S.; Rossano, L. T. U.S. 5,130,439; 1992.
17. Irani, R. J.; SantaLucia, J., Jr. *Nucleosides Nucleotides Nucleic Acids* **2002**, *21*, 737.
18. Hulin, B.; Clark, D. A.; Goldstein, S. W.; McDermott, R. E.; Dambek, P. J.; Kappeler, W. H.; Lamphere, C. H.; Lewis, D. M.; Rizzi, J. P. *J. Med. Chem.* **1992**, *35*, 1853.
19. Casimiro-Garcia, A.; Bigge, C. F.; Davis, J. A.; Padalino, T.; Pulaski, J.; Ohren, J. F.; McConnell, P.; Kane, C. D.; Royer, L. J.; Stevens, K. A.; Auerbach, B. J.; Collard, W. T.; McGregor, C.; Fakhoury, S. A.; Schaum, R. P.; Zhou, H. *Bioorg. Med. Chem.* **2008**, *16*, 4883.
20. Casimiro-Garcia, A.; Bigge, C. F.; Davis, J. A.; Padalino, T.; Pulaski, J.; Ohren, J. F.; McConnell, P.; Kane, C. D.; Royer, L. J.; Stevens, K. A.; Auerbach, B.; Collard, W.; McGregor, C.; Song, K. *Bioorg. Med. Chem.* **2009**, *17*, 7113.
21. Structure deposited in the RCSB Protein Data Bank under PDB ID: 4HEE. X-ray data collection data and structure refinement statistics can be found in the [Supplementary data](#).
22. Experimental Log*D* determined using octanol/buffer shake flask method.
23. Kinetic solubility measured in 100 mM potassium phosphate pH 6.5 buffer.
24. Drug–drug interaction: % inhibition of selected cytochrome P450 isoform with a compound concentration of 3 μM.